JSHC
Japan Society of
Histochemistry and Cytochemistry
Established 1959

Acta Histochem. Cytochem. 49 (3): 89–95, 2016
doi: 10.1267/ahc.16005

Aquaporin-4 Protein Is Stably Maintained in the Hypertrophied Muscles by Functional Overload

Minenori Ishido[1] and Tomohiro Nakamura[1]

[1]*Section for Health-related Physical Education, Division of Human Sciences, Faculty of Engineering, Osaka Institute of Technology, Osaka 535–8585, Japan*

Received March 1, 2016; accepted May 19, 2016; published online June 16, 2016

Aquaporin-4 (AQP4) is a selective water channel that is located on the plasma membrane of myofibers in skeletal muscle and is bound to α1-syntrophin. It is considered that AQP4 is involved in the modulation of homeostasis in myofibers through the regulation of water transport and osmotic pressure. However, it remains unclear whether AQP4 expression is altered by skeletal muscle hypertrophy to modulate water homeostasis in myofibers. The present study investigated the effect of muscle hypertrophy on the changes in AQP4 and α1-syntrophin expression patterns in myofibers. Novel findings indicated in the present study were as follows: 1) Expression levels of AQP4 and α1-syntrophin were stably maintained in hypertrophied muscles, and 2) AQP4 was not expressed in the myofibers containing the slow-type myosin heavy chain isoform (MHC) with or without the presence of fast-type MHC. The present study suggests that AQP4 may regulate the efficiency of water transport in hypertrophied myofibers through its interaction with α1-syntrophin. In addition, this study suggests that AQP4 expression may be inhibited by a regulatory mechanism activated under physiological conditions that induces the expression of slow-type MHC in skeletal muscles.

Key words: aquaporin-4, α1-syntrophin, skeletal muscle, hypertrophy

I. Introduction

Aquaporin is a selective water channel that is located on the plasma membrane of various kinds of cells, and is considered to play an important role in the movement of molecular water to modulate the osmotic pressure within cells [15, 19, 20, 21]. In particular, aquaporin-4 (AQP4) is the sole water channel present in mammalian skeletal muscle *in vivo* [5, 8]. On the plasma membrane of myofibers, AQP4 stabilizes binds to α1-syntrophin, which is a component of the dystrophin-associated protein complex in skeletal muscle, and thus, it is thought that α1-syntrophin plays an important role in regulating AQP4 expression in skeletal muscle [1, 17, 25]. Interestingly, in skeletal muscle, AQP4 is selectively expressed in fast-twitch myofibers but not in slow-twitch myofibers, and thus it is considered that the expression of AQP4 is dependent on the manner of recruitment of myofibers [5, 7, 13].

AQP4 mediates water transport between blood and myofibers for the modulation of rapid volume changes that occur during muscle contraction, and, together with aquaporin-1, is expressed on microvessels [8]. Moreover, in addition to modulating the osmotic pressure in myofibers, it has been suggested that AQP4 is involved in the regulation of myofiber energy metabolism [2]. Furthermore, as the expression of AQP4 is markedly reduced or absent in dystrophic muscles with dystrophin deficiency, it has also been suggested that AQP4-mediated water homeostasis is involved in the pathological process of muscular dystrophy [4, 6, 9, 16, 22]. On the other hand, pathologic findings, such as edema, were not detected in the morphology of skeletal muscles in AQP4 overexpressing transgenic mice [23]. Moreover, it is reported that muscle strength, osmotic water permeability, and the contents of the water in skeletal muscle were not altered in AQP4 knockout mice, compared with wild-type mice [24]. Thus, there is no consensus on the physiological role of AQP4 in the maintenance of skel-

Correspondence to: Minenori Ishido, Division of Human Sciences, Osaka Institute of Technology, Ohmiya, Asahi-ku, Osaka 535–8585, Japan.
E-mail: minenori.ishido@oit.ac.jp

etal muscle homeostasis *in vivo*. In particular, to the best of our knowledge, the physiological role of AQP4 in the regulation of the morphology of skeletal muscles has not been investigated, and thus, it remains unclear whether skeletal muscle hypertrophy is accompanied by the alteration of AQP4 expression to modulate the efficiency of water transport in myofibers *in vivo*. In addition, it remains unclear whether the alteration of the expression of AQP4 and α1-syntrophin is synchronized during skeletal muscle hypertrophy. Therefore, the present study investigated the alteration of AQP4 and α1-syntrophin expression levels in hypertrophied skeletal muscle *in vivo*, to provide a molecular basis to elucidate its physiological role in the regulation of morphological changes in skeletal muscle *in vivo*.

II. Materials and Methods

Experimental design and surgical procedure

Adult female Fischer 344 rats (8 weeks of age) were used in this study, and randomly assigned to control (C) and overload (Ov) groups (n=6 per group). The rats were housed in individual cages at 22°C, with a 12 hr light/dark cycle and were provided with food and water ad libitum. All experiments were carried out with the approval of the Ethics Committee on Life Sciences of Osaka Institute of Technology.

In order to produce overload-induced muscle hypertrophy of the plantaris muscle, ablation of the ipsilateral synergistic gastrocnemius and soleus muscles was performed as described previously [10–12]. Briefly, under pentobarbital sodium anesthesia (60 mg kg-1 i.p.), a skin incision was made to fully expose the dorsal region of the experimental leg. The soleus muscle was completely removed except for a small portion at the proximal end, where it attaches to the plantaris. Both the lateral and medial gastrocnemius muscles were completely removed. Contralateral plantaris muscles were used as sham-operated controls (C group) because there was no significant difference between the sham-operated and sedentary muscle (data not shown). The animals were sacrificed at 5 weeks post-surgery. At the time of death, each rat was anesthetized and the plantaris muscles were removed. The samples were quickly frozen in liquid nitrogen and stored at −80°C until use.

Immunohistochemical analysis

For immunostaining, serial cross-sections (10 μm thick) of mid-belly muscles were cut using a cryostat at −20°C and thawed on 3-amino propylethoxysilane-coated slides. The sections were fixed with 4% paraformaldehyde in 0.1 M phosphate buffer solution (pH 7.4) for 15 min and washed with 0.1 M phosphate-buffered saline (PBS, pH 7.4). Then, to block any nonspecific immunoreactivity, the sections were incubated with 0.1 M PBS containing 10% normal serum and 1% Triton X-100 for 1 hr. The primary antibodies were diluted with 0.1 M PBS containing 5% normal serum and 0.3% Triton X-100, and the secondary antibodies were diluted with 0.1 M PBS containing 5% normal serum and 0.1% Triton X-100.

For multicolor immunofluorescence staining, the sections were simultaneously incubated for 16–48 hr at 4°C with the primary antibodies. The primary antibodies used in the present study were as follows: goat polyclonal anti-AQP4 (1:400; Santa Cruz Biotech, Santa Cruz, CA, USA), mouse monoclonal anti-Dystrophin (1:100; Sigma, St Louis, MO, USA), mouse monoclonal anti-Pax7 (1:100; R&D systems, Inc. Minneapolis, MN, USA), mouse monoclonal anti-Myosin (skeletal, fast) (1:100; Sigma) and mouse monoclonal anti-Myosin (skeletal, slow) (1:100; Sigma). Then, the sections were washed in 0.1 M PBS, and simultaneously incubated overnight at 4°C with secondary antibodies. The secondary antibodies used in the present study were fluorescein-labeled horse anti-mouse IgG (1:300, Vector Laboratories, Burlingame, CA, USA) and the Alexa Fluor 568-labeled donkey anti-goat IgG (1:300; Molecular Probes, Eugene, OR, USA). Then, the sections were washed in 0.1 M PBS and mounted in VECTASHIELD Mounting Medium with DAPI (Vector Laboratories) to visualize the nuclei. All image analyses were performed using a fluorescence microscope (BX60; Olympus, Tokyo, Japan) and a Penguin 600CL (Pixera Corporation, CA, USA).

Western blot analysis

Cryosections, 250 μm thick, (25 sections × 10 μm thick) of mid-belly muscles were cut using a cryostat at −20°C and were homogenized in 300 μl of RIPA buffer (50 mM Tris-HCl pH 8.0, 150 mM sodium chloride, 1% NP-40, 0.5% sodium deoxycholate, and 0.1% sodium dodecyl sulfate) (Sigma) containing 1× Protease Inhibitor Cocktail (Roche Diagnostic). After the homogenate samples were centrifuged at 12000×g for 10 min at 4°C, the supernatant fluids were collected.

The homogenate samples were resolved by SDS-PAGE (12.5% polyacrylamide gel) and transferred onto polyvinylidene difluoride membranes (ATTO, Tokyo, Japan) at 144 mA for 45 min. After transfer, to block any nonspecific immunoreactivity, the membranes were incubated with 20 mM Tris-buffered saline (TBS) (pH 7.6) containing 5% normal serum and 0.1% Tween-20 for 1 hr at room temperature. The membranes were then incubated overnight at 4°C with primary antibodies. The primary antibodies were diluted with 20 mM TBS containing 5% normal serum and 0.1% Tween-20. The primary antibodies used in the present study were as follows: goat polyclonal anti-AQP4 (1:500; Santa Cruz), mouse monoclonal Anti-β-Actin (internal control, 1:2000; Abcam, Cambridge, UK), rabbit polyclonal Anti-Syntrophin alpha 1 (1:4000; Abcam). Then, they were washed in 20 mM TBS containing 5% normal serum and 0.1% Tween-20, and incubated for 1 hr at room temperature with secondary antibodies. The secondary antibodies used in the present study were as follows: biotinylated anti-mouse IgG (1:10000; Vector

Labs, Burlingame, CA, USA), biotinylated anti-rabbit IgG (1:10000; invitrogen, Camarillo, CA, USA), biotinylated anti-goat IgG (1:10000; Millipore, Temecula, CA, USA). They were washed in 20 mM TBS containing 5% normal serum and 0.1% Tween-20, and incubated for 1 hr at room temperature with TBS containing 5% normal serum and peroxidase conjugated streptavidin horseradish (1:50000; GE Healthcare, Buckinghamshire, UK). Finally, immunoreactivity was detected by chemiluminescence using ImmunoStar LD (Wako, Osaka, Japan). The bands were quantified by densitometric analysis using ImageJ software (ver.1.48, http://rsb.info.nih.gov/ij/). The mean value for the control samples on each immunoblot, expressed relative to β-actin as an internal control, was adjusted to equal 1.0, and each sample value was expressed relative to the adjusted mean value for the control group.

Analysis of the myofiber cross-sectional area in response to functional overload

For the evaluation of the myofiber cross-sectional area in response to functional overload, serial cross sections (10 μm thick) of mid-belly muscles were cut using a cryostat (CM3050, Leica, Germany) at −20°C and thawed on 3-amino propylethoxysilane-coated slides. Then, these sections were visualized using hematoxylin and eosin (HE) staining. As described previously [3], to calculate the mean myofiber cross-sectional area in each sample, at least 30 photographs covering the entire muscle section were taken for each sample. Furthermore, the cross-sectional areas of at least 400 myofibers were randomly measured in each sample using ImageJ software.

Statistical analysis

All data are represented as means±SD and were analyzed using the StatView statistical-analysis program (SAS institute Inc., Cary, NC, USA). Differences between C and Ov groups were tested by one-way ANOVA using Scheffé's S test. Differences were considered to be significant at the confidence level of 0.05.

III. Results

The relative plantaris muscle weight in the Ov group was significantly higher than that in the C group ($p<0.05$) (Fig. 1). Furthermore, the mean cross-sectional area of the myofibers in the Ov group was significantly higher than that in the C group ($p<0.05$) (Fig. 2). Therefore, these results indicate that myofiber hypertrophy was induced by functional overload.

Localization of AQP4 in normal skeletal muscle

We observed the ring-like expression pattern of AQP4-positive immunoreactivity throughout contralateral control muscles (Fig. 3A–C). Then, it was detected that AQP4-positive immunoreactivity was colocalized with dystrophin-positive immunoreactivity (Fig. 3D–G). Therefore, these findings indicate that the expression of AQP4 is localized on the plasma membrane of myofibers.

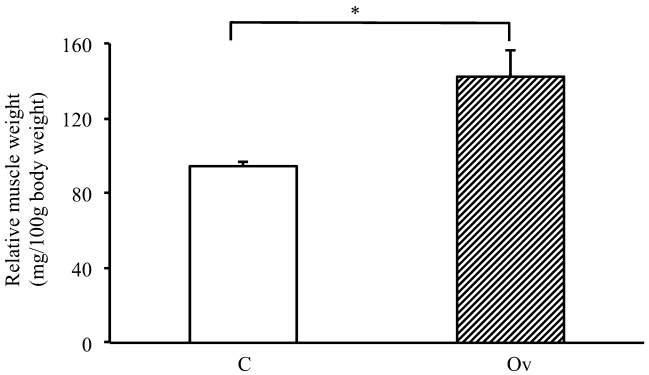

Fig. 1. Relative muscle weight in control and overloaded plantaris muscles. Values are means±SD. Relative muscle weight is presented as mg/100g body weight. C: contralateral sham-operated muscles. Ov: overloaded muscles. *Significant difference between C and O group ($p<0.05$).

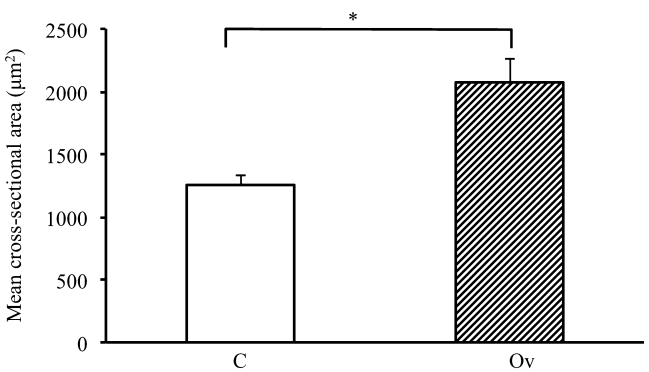

Fig. 2. Mean cross-sectional area of the myofibers in contralateral sham-operated and overloaded plantaris muscles. Values are means±SD. C: control muscles. Ov: overloaded muscles. *Significant difference between C and Ov group ($p<0.05$).

Next, to clarify whether AQP4 is expressed on skeletal muscle satellite cells, we performed double fluorescence immunohistochemical staining using Pax7 and AQP4 antibodies on contralateral control muscles (Fig. 4A–D). APQ4-positive immunoreactivity was not detected on the Pax7-positive satellite cells. Thus, this finding indicates that AQP4 is not expressed on skeletal muscle satellite cells.

Relationship between AQP4 expression patterns and myosin heavy chain expression patterns in myofibers

In vivo skeletal muscle is composed of several types of myofibers, e.g. MHC-F (+)/MHC-S (−), MHC-F (−)/MHC-S (+), and MHC-F (+)/MHC-S (+) myofibers. The present study investigated the relationship among the expression patterns of AQP4, MHC-F, and MHC-S in skeletal muscle. As shown in Fig. 5 (A–C), in contralateral control muscles, AQP4-positive immunoreactivity was detected with MHC-

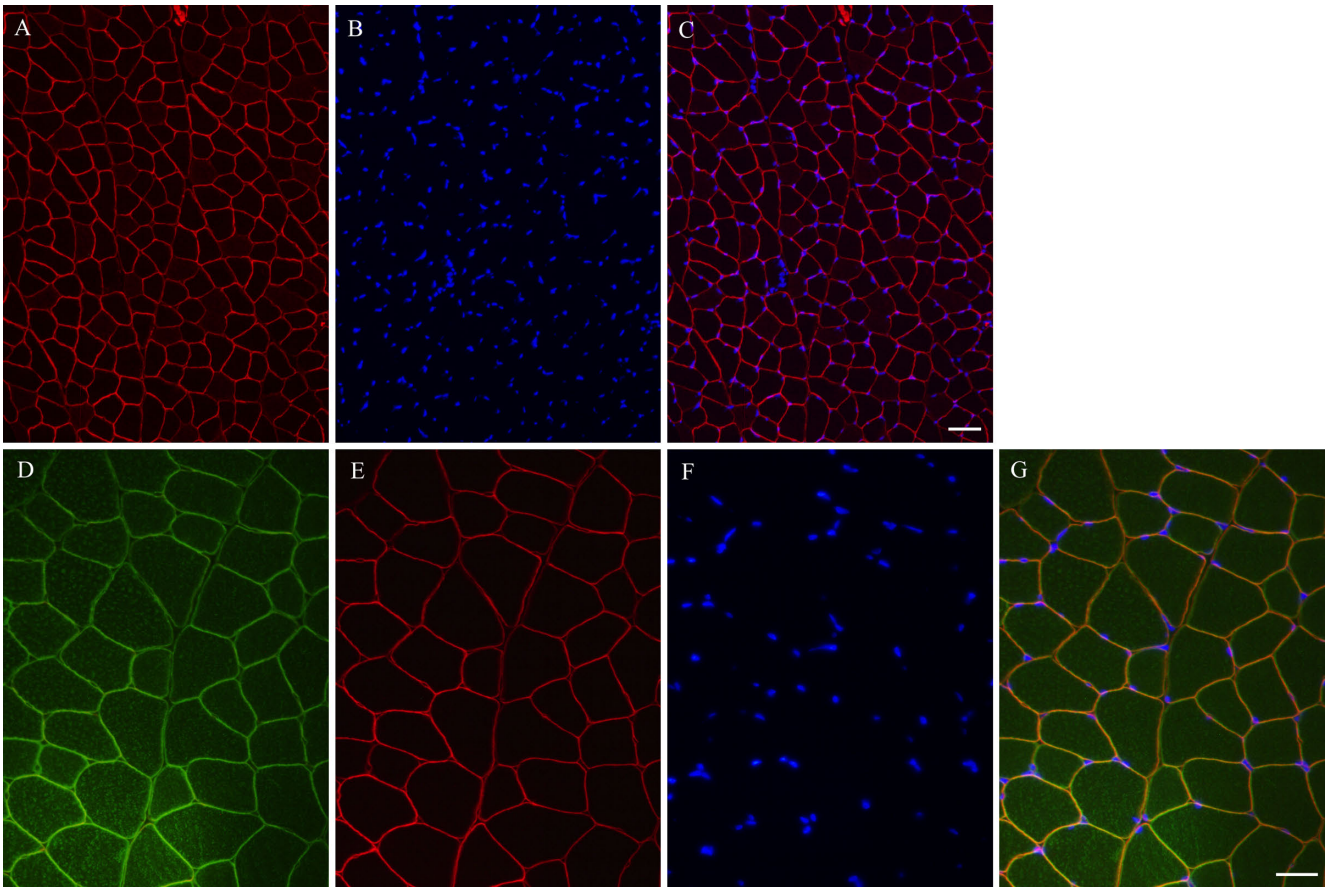

Fig. 3. Photomicrographs showing the localization of AQP4 in control plantaris muscles. Immunostaining was performed to visualize the localization of AQP4 (**A**) and nuclei (**B**), and the two images were merged (**C**). Immunostaining was performed to visualize the localization of dystrophin (**D**), AQP4 (**E**), and nuclei (**F**), and the three images were merged (**G**). Bar=50 μm (**A–C**) and 30 μm (**D–G**).

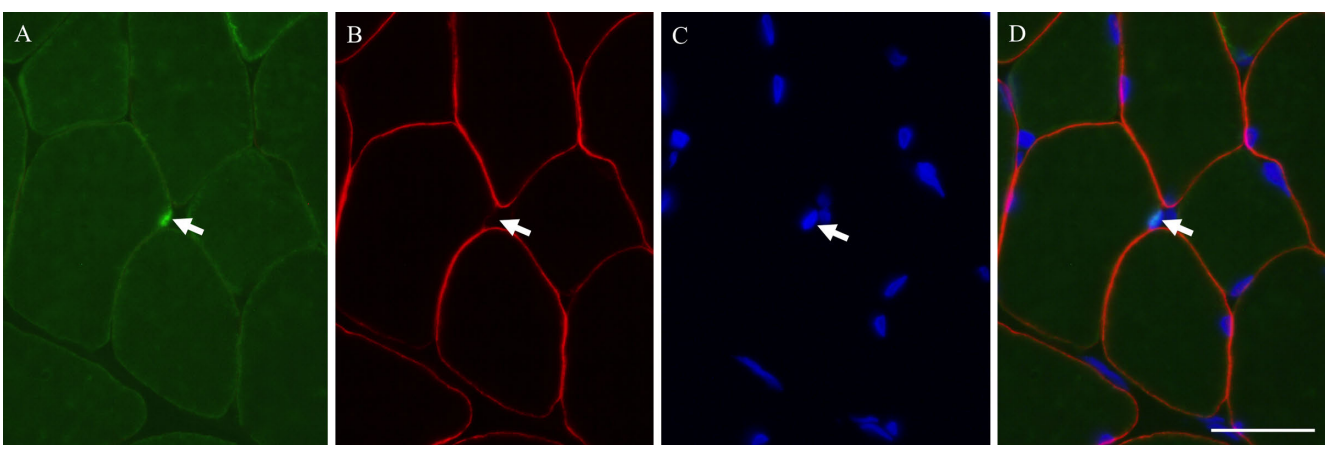

Fig. 4. Photomicrographs showing no expression of AQP4 in satellite cells in control plantaris muscles. Immunostaining was performed to visualize the localization of Pax7 (**A**), AQP4 (**B**), and nuclei (**C**), and the three images were merged (**D**). The arrow (**A–D**) indicates no expression of AQP4 in Pax7-positive satellite cells. Bar=30 μm (**A–D**).

F (+)/MHC-S (−) myofibers. Conversely, AQP4-positive immunoreactivity was not detected in MHC-F (−)/MHC-S (+) myofibers. MHC-F (+)/MHC-S (+) myofibers were not detected in contralateral control muscles (data not shown). On the other hand, MHC-F (+)/MHC-S (+) myofibers were detected in the skeletal muscles exposed to functional overload, and furthermore, in these myofibers, AQP4-positive immunoreactivity was not observed (Fig. 5D–F). Thus, these findings indicate a relationship among AQP4, MHC-F, and MHC-S expression patterns in skeletal muscle.

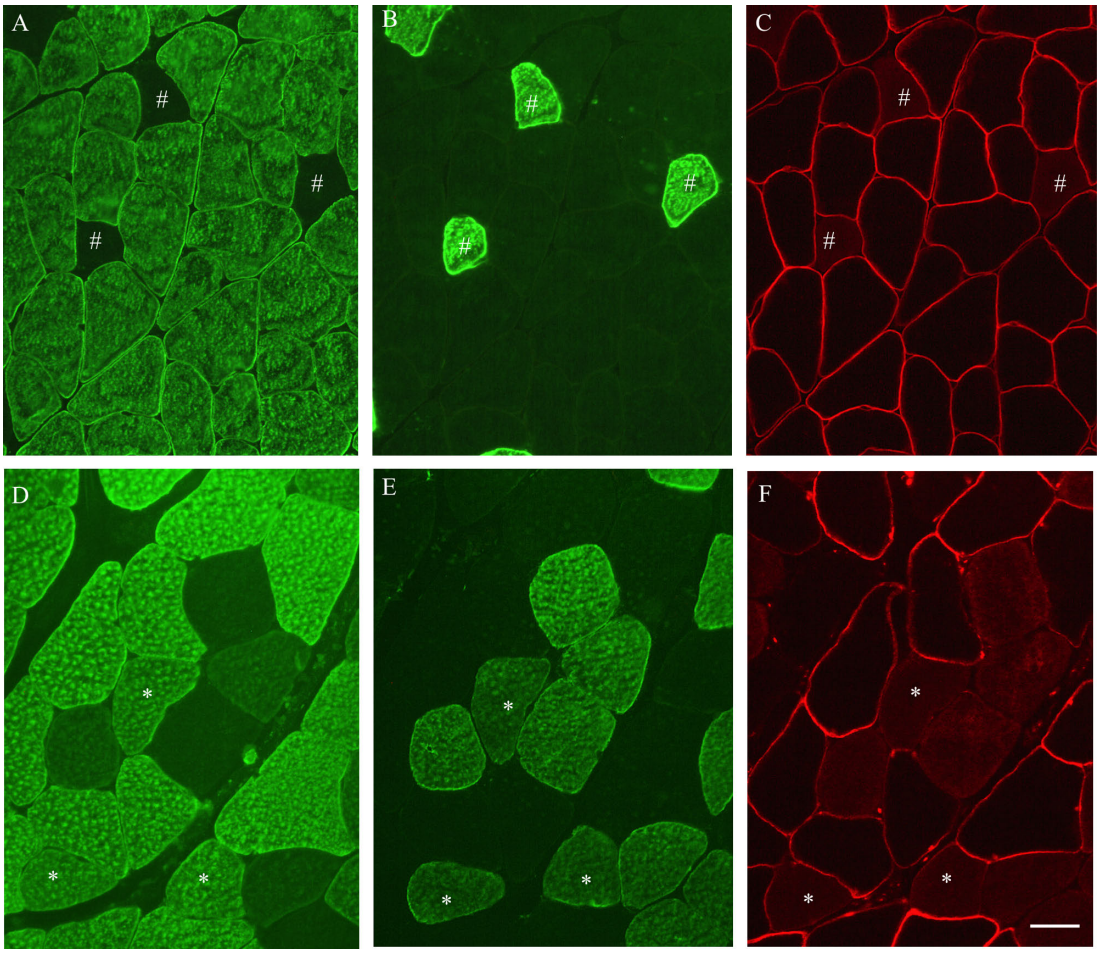

Fig. 5. Photomicrographs showing the relationship between myosin heavy chain isoforms and AQP4 in control and overloaded plantaris muscles. Immunostaining was performed to visualize the localization of MHC-F (**A, D**), MHC-S (**B, E**), and AQP4 (**C, F**) using serial cross-sections. In control muscles (**A–C**), MHC-F (+)/MHC-S (−) myofibers (non symbol) indicated AQP4-positive immunoreactivity, and MHC-F (−)/MHC-S (+) myofibers (#) indicated AQP4-negative immunoreactivity. There was no MHC-F (+)/MHC-S (+) myofiber. In overloaded muscles (**D–F**), MHC-F (+)/MHC-S (+) myofibers (*) indicated AQP4-negative immunoreactivity. Bar=30 μm.

Effect of skeletal muscle hypertrophy in AQP4 and α1-syntrophin proteins

To investigate changes in the expression of AQP4 and α1-syntrophin proteins with regard to skeletal muscle hypertrophy, we performed western blot analysis using AQP4 and α1-syntrophin antibodies, respectively (Fig. 6A). The expression level of AQP4 in the Ov group was similar to that in the C group (Fig. 6B). In addition, there was no significant difference between the expression levels of α1-syntrophin protein in the C and Ov group (Fig. 6C). These findings indicate that the expression level of AQP4 and α1-syntrophin proteins in skeletal muscle subjected to functional overload was relatively unchanged, compared with normal skeletal muscle.

IV. Discussion

The expression of AQP4 is decreased in mammalian skeletal muscle with muscular dystrophy, and thus it is suggested that AQP4 contributes to the regulation of skeletal muscle morphology [6, 9, 22]. However, it remains unclear whether the expression of AQP4 changes in response to morphological changes in normal skeletal muscle. The present study indicated that changes in AQP4 expression were involved in functional overload-induced skeletal muscle hypertrophy, and suggested a relationship between the expression level of AQP4 and the size of myofibers.

The present study showed that the expression of AQP4 is localized on the dystrophin-positive plasma membrane of myofibers, and this result corresponded to the localization of AQP4 in skeletal muscle found in the previous studies [13, 14]. On the other hand, although it remains unclear whether AQP4 is localized in skeletal muscle satellite cells *in vivo* until now, we have first demonstrated that satellite cells do not express AQP4 in skeletal muscle.

One of the characteristics of AQP4 expression patterns in skeletal muscle is the relevance of the type of MHC in the myofibers. Previous studies have shown that myofibers

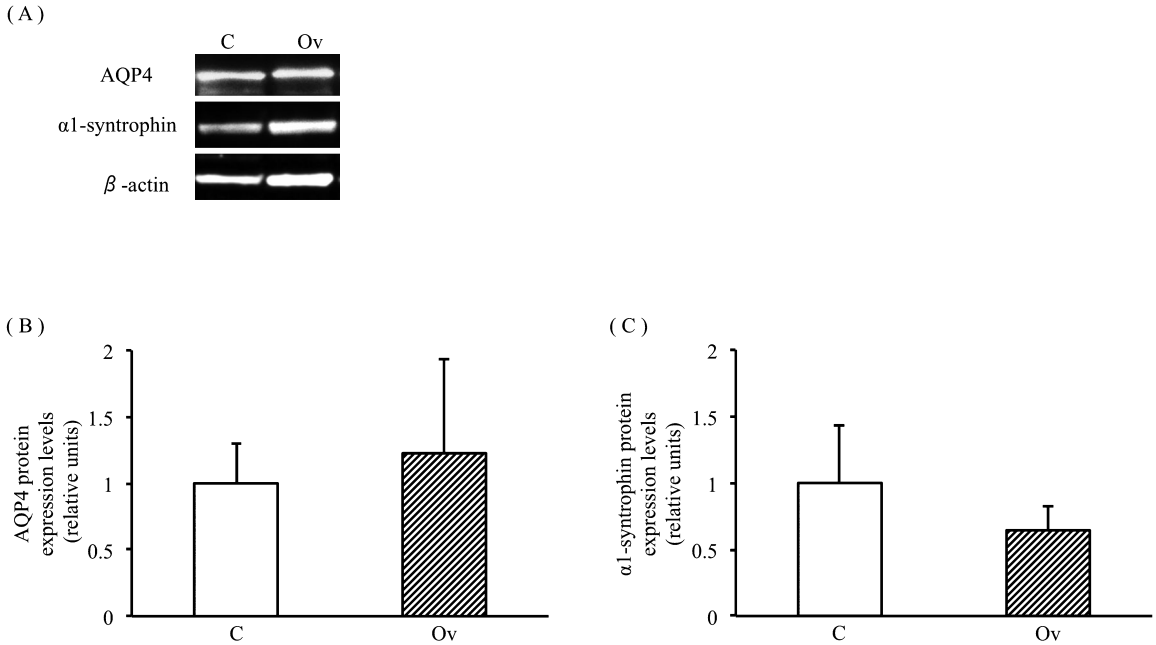

Fig. 6. AQP4 and α1-syntrophin protein expression in contralateral sham-operated and overloaded plantaris muscles. (**A**) The levels of AQP4, α1-syntrophin, and β-actin protein were analyzed by Western blot. β-actin was used as an internal control. (**B**) AQP4 protein expression levels, normalized for β-actin protein expression levels, were calculated by densitometric analysis. (**C**) α1-syntrophin protein expression levels, normalized for β-actin protein expression levels, were calculated by densitometric analysis. Values are means±SD. C: control muscles. Ov: overloaded muscles. Fold change was expressed relative to the levels observed in the C group. In the expression levels of AQP4 and α1-syntrophin protein, there were no significant differences between C and Ov groups, respectively.

expressing AQP4 had MHC-F, whereas AQP4 was not expressed in myofibers that had MHC-S but no MHC-F [5, 18, 23, 24]. Thus, it has been suggested that the regulation of AQP4 expression may depend on muscle activities that promote the expression of MHC-F [7]. However, these previous studies did not investigate the expression pattern of AQP4 in MHC-F (+)/MHC-S (+) myofibers. In the present study, we first demonstrated the expression of AQP4 was not detected on MHC-F (+)/MHC-S (+) myofibers in functional overloaded skeletal muscle although there were no MHC-F (+)/MHC-S (+) myofibers in normal control muscles. Therefore, in contrast to previous suggestion, the present study provides a novel hypothesis that the expression of AQP4 may be inhibited under physiological conditions that induce the expression of MHC-S in skeletal muscles, with or without the presence of MHC-F. Further investigation is needed to elucidate the relationship between the expression pattern of AQP4 and the types of myofibers in skeletal muscle.

The relationship between the changes in the AQP4 expression level and the morphological change of skeletal muscle remains unknown, until now. We first demonstrated that the expression level of AQP4 in the hypertrophied skeletal muscles was maintained, compared with the contralateral control muscles. Furthermore, as well as with AQP4, the relative expression level of α1-syntrophin, in the hypertrophied skeletal muscles, was not significantly altered compared with that in contralateral control muscles. In general, because AQP4 is localized under the plasma membrane through an α1-syntrophin-mediated interaction, the regulation of AQP4 expression is associated closely with the expression of α1-syntrophin [1, 17, 25]. However, it remains unclear whether the changes in the expression of AQP4 are correlated with the changes in expression of α1-syntrophin. We first demonstrated a relationship between AQP4 and α1-syntrophin expression levels in hypertrophied skeletal muscles similar to control muscles. Moreover, in the present study, the mean cross-sectional area of the myofibers in overloaded muscles was significantly higher than that in contralateral control muscles. Therefore, the efficiency of water transport and osmotic pressure may be maintained in myofibers by the modulation of the expression levels of AQP4 and α1-syntrophin in response to myofiber hypertrophy. Although the functional significance of AQP4 in the morphological changes in skeletal muscle *in vivo* is not fully understood, in the present study, we suggest that AQP4 might be involved in the regulation of skeletal muscle hypertrophy through its interaction with α1-syntrophin. In the future, further investigation is needed to elucidate the molecular mechanism(s) regulating the expression level of AQP4 during muscle hypertrophy.

In conclusion, the present study demonstrated that the expression of AQP4 was absent in the myofibers expressing MHC-S with or without the expression of MHC-F in skeletal muscles. Moreover, we first found that the relative expression level of AQP4 in hypertrophied skeletal muscles

was maintained at a level similar to control muscles, and this phenomenon was accompanied by the modulation of the expression level of α1-syntrophin. Therefore, the present study suggests that AQP4 plays an important role in regulating muscle hypertrophy through its interaction with α1-syntrophin in response to functional overload.

V. References

1. Adams, M. E., Mueller, H. A. and Froehner, S. C. (2001) *In vivo* requirement of the alpha-syntrophin PDZ domain for the sarcolemmal localization of nNOS and aquaporin-4. *J. Cell Biol.* 155; 113–122.
2. Basco, D., Nicchia, G. P., D'Alessandro, A., Zolla, L., Svelto, M. and Frigeri, A. (2011) Absence of aquaporin-4 in skeletal muscle alters proteins involved in bioenergetic pathways and calcium handling. *PLoS One* 6; e19225.
3. Chaillou, T., Koulmann, N., Simler, N., Meunier, A., Serrurier, B., Chapot, R., Peinnequin, A., Beaudry, M. and Bigard, X. (2012) Hypoxia transiently affects skeletal muscle hypertrophy in a functional overload model. *Am. J. Physiol. Regul. Integr. Comp. Physiol.* 302; R643–654.
4. Crosbie, R. H., Dovico, S. A., Flanagan, J. D., Chamberlain, J. S., Ownby, C. L. and Campbell, K. P. (2002) Characterization of aquaporin-4 in muscle and muscular dystrophy. *FASEB J.* 16; 943–949.
5. Frigeri, A., Nicchia, G. P., Verbavatz, J. M., Valenti, G. and Svelto, M. (1998) Expression of aquaporin-4 in fast-twitch fibers of mammalian skeletal muscle. *J. Clin. Invest.* 102; 695–703.
6. Frigeri, A., Nicchia, G. P., Nico, B., Quondamatteo, F., Herken, R., Roncali, L. and Svelto, M. (2001) Aquaporin-4 deficiency in skeletal muscle and brain of dystrophic mdx mice. *FASEB J.* 15; 90–98.
7. Frigeri, A., Nicchia, G. P., Desaphy, J. F., Pierno, S., De Luca, A., Camerino, D. C. and Svelto, M. (2001) Muscle loading modulates aquaporin-4 expression in skeletal muscle. *FASEB J.* 15; 1282–1284.
8. Frigeri, A., Nicchia, G. P., Balena, R., Nico, B. and Svelto, M. (2004) Aquaporins in skeletal muscle: reassessment of the functional role of aquaporin-4. *FASEB J.* 18; 905–907.
9. Hara, H., Wakayama, Y., Kojima, H., Inoue, M., Jimi, T., Iijima, S. and Masaki, H. (2011) Aquaporin 4 expression in the mdx mouse diaphragm. *Acta Histochem. Cytochem.* 44; 175–182.
10. Ianuzzo, C. D. and Chen, V. (1977) Compensatory hypertrophy of skeletal muscle: contractile characteristics. *Physiol. Teach.* 6; 4–7.
11. Ishido, M. and Kami, K. (2004) Localization of MyoD, myogenin and cell cycle regulatory factors in hypertrophying rat skeletal muscles. *Acta Physiol. Scand.* 180; 281–289.
12. Ishido, M., Uda, M., Kasuga, N. and Masuhara, M. (2009) The expression patterns of Pax7 in satellite cells during overload-induced rat adult skeletal muscle hypertrophy. *Acta Physiol (Oxf).* 195; 459–469.
13. Kaakinen, M., Salmela, P., Zelenin, S. and Metsikko, K. (2007) Distribution of aquaporin 4 on sarcolemma of fast-twitch skeletal myofibres. *Cell Tissue Res.* 329; 529–539.
14. Kaakinen, M., Zelenin, S. and Metsikko, K. (2011) Aquaporin-4 water channel oligomers are associated with the transverse tubules of skeletal myofibers. *Exp. Cell Res.* 317; 20–28.
15. Kozono, D., Yasui, M., King, L. S. and Agre, P. (2002) Aquaporin water channels: atomic structure molecular dynamics meet clinical medicine. *J. Clin. Invest.* 109; 1395–1399.
16. Liu, J. W., Wakayama, Y., Inoue, M., Shibuya, S., Kojima, H., Jimi, T. and Oniki, H. (1999) Immunocytochemical studies of aquaporin 4 in the skeletal muscle of mdx mouse. *J. Neurol. Sci.* 164; 24–28.
17. Neely, J. D., Amiry-Moghaddam, M., Ottersen, O. P., Froehner, S. C., Agre, P. and Adams, M. E. (2001) Syntrophin-dependent expression and localization of Aquaporin-4 water channel protein. *Proc. Natl. Acad. Sci. U S A* 98; 14108–14113.
18. Nicchia, G. P., Mola, M. G., Pisoni, M., Frigeri, A. and Svelto, M. (2007) Different pattern of aquaporin-4 expression in extensor digitorum longus and soleus during early development. *Muscle Nerve* 35; 625–631.
19. Preston, G. M. and Agre, P. (1991) Isolation of the cDNA for erythrocyte integral membrane protein of 28 kilodaltons: member of an ancient channel family. *Proc. Natl. Acad. Sci. U S A* 88; 11110–11114.
20. Preston, G. M., Carroll, T. P., Guggino, W. B. and Agre, P. (1992) Appearance of water channels in Xenopus oocytes expressing red cell CHIP28 protein. *Science* 256; 385–387.
21. Verkman, A. S. and Mitra, A. K. (2000) Structure and function of aquaporin water channels. *Am. J. Physiol. Renal. Physiol.* 278; F13–28.
22. Wakayama, Y., Jimi, T., Inoue, M., Kojima, H., Murahashi, M., Kumagai, T., Yamashita, S., Hara, H. and Shibuya, S. (2002) Reduced aquaporin 4 expression in the muscle plasma membrane of patients with Duchenne muscular dystrophy. *Arch. Neurol.* 59; 431–437.
23. Wakayama, Y., Takahashi, J., Shibuya, S., Inoue, M., Kojima, H., Oniki, H., Arata, S., Hara, H., Jimi, T., Shioda, S., Sunada, Y., Ohi, H. and Shimizu, T. (2007) Generation of muscle aquaporin 4 overexpressing transgenic mouse: its characterization at RNA and protein levels including freeze-fracture study. *Micron* 38; 257–267.
24. Yang, B., Verbavatz, J. M., Song, Y., Vetrivel, L., Manley, G., Kao, W. M., Ma, T. and Verkman, A. S. (2000) Skeletal muscle function and water permeability in aquaporin-4 deficient mice. *Am. J. Physiol. Cell Physiol.* 278; C1108–C1115.
25. Yokota, T., Miyagoe, Y., Hosaka, Y., Tsukita, K., Kameya, S., Shibuya, S., Matsuda, R., Wakayama, Y. and Takeda, S. (2000) Aquaporin-4 is absent at the sarcolemma and at perivascular astrocyte endfeet in α1-syntrophin knockout mice. *Proc. Japan Acad.* 76; 22–27.